Current Biology, Vol. 15, 453–458, March 8, 2005, ©2005 Elsevier Ltd All rights reserved. DOI 10.1016/j.cub.2004.12.081

Perceiving Time to Collision Activates the Sensorimotor Cortex

David T. Field and John P. Wann*
School of Psychology
University of Reading
Earley Gate
Reading RG6 6AL
United Kingdom

Summary

The survival of many animals hinges upon their ability to avoid collisions with other animals or objects, or to precisely control the timing of collisions. Optical expansion provides a compelling impression of object approach and in principle can provide the basis for judgments of time to collision (TTC) [1]. It has been demonstrated that pigeons [2] and houseflies [3] have neural systems that can initiate rapid coordinated actions on the basis of optical expansion. In the case of humans, the linkage between judgments of TTC and coordinated action has not been established at a cortical level. Using functional magnetic resonance imaging (fMRI), we identified superior-parietal and motor-cortex areas that are selectively active during perceptual TTC judgments, some of which are normally involved in producing reach-to-grasp responses. These activations could not be attributed to actual movement of participants. We demonstrate that networks involved in the computational problem of extracting TTC from expansion information have close correspondence with the sensorimotor systems that would be involved in preparing a timed motor response, such as catching a ball or avoiding collision.

Results

Human performers on the highway, pavement, or sports field need to tune their actions with respect to the time to collision (TTC) of an approaching object. To make an accurate judgment of TTC, one does not need to estimate object velocity or distance because, for sufficiently large, nonaccelerating objects approaching the eye, information about the immediacy of the impending collision is available from the ratio of the current expansion rate and retinal image size [1, 4, 5]. It has been demonstrated that area MT+ in the visual cortex is sensitive to optic expansion [6], but we have little knowledge of what areas are involved in deriving the higher-order percept of TTC from the joint processing of optical size and expansion rate. Here, we used fMRI to reveal the neural correlates of processing TTC from image expansion while controlling for those areas that are selectively activated by expansion alone. When an object approaches the point of observation, it presents an accelerating pattern of optical expansion. The presence of retinal-image expansion will produce a strong response in the primary visual cortex. We isolated areas that were active only during TTC processing by using a control task that required judgment of the expansion rate of inflating objects that were fixed in depth and did not appear to approach the observer.

Our main TTC task was based upon one used previously by Todd [7]. Two spheres approached the point of observation, one either side of the midline, and the arrival time of one object was delayed by 200 ms with respect to the other. Observers decided which of the two objects would arrive first and responded by pressing a button on a hand-held box as soon as they were confident in their judgment (Figure 1A). In our inflation judgment task (IJ), two oval objects were shown suspended on a fixed-size frame indicating a fixed depth in the world. The objects inflated in size asymmetrically, and observers judged which object was expanding faster; they responded by pressing a button identical to that in the TTC task as soon as they were confident in their judgment (Figure 1B). The relevant optical variable for successful performance in the TTC task was the ratio of image size to expansion rate, whereas in the IJ task it was expansion rate independent of image size. In a variant TTC task, observers were presented with two remote objects translating in the frontoparallel plane, and they were required to judge which would arrive first at a central target location (Figure 1C). In common with the TTC task, this required the joint processing of two optical variables, gap angle and rate of closure, to judge the arrival time, but image expansion, motion in depth, and movement toward the point of observation were all absent. The inclusion of this gap-closure (GC) condition allowed us to determine to what extent the cortical areas identified by our main contrast were specific to the processing of TTC from image expansion or reflected a more generalized processing of relative motion variables.

Twelve participants were scanned in a Siemens 3T scanner while performing the TTC, IJ, and GC tasks as well as while in a resting baseline condition. The accuracy of judgments in the three experimental conditions was equivalent (percent correct: TTC, 86%; IJ, 83%; and GC, 82%. $F_{(2,22)} = 0.89$, $p = 0.42$, not significant [NS]), so the three tasks were well matched in terms of difficulty, which therefore cannot account for the differences in the blood-oxygen-level-dependent (+) signal between the three conditions.

We first subtracted the resting baseline activation from that in the TTC task (Figure 2; see also Table S1 in the Supplemental Data online). This revealed activation in the primary visual cortex, especially in the motion-sensitive area MT+, as well as substantial activity in the occipitoparietal dorsal stream. Bilateral dorsal-stream activation was observed in both the anterior and posterior intraparietal sulcus (IPS) and was also observed to run the length of the postcentral sulcus (postCS). Activation also extended into motor cortex, with only the left hemisphere showing activation in the central sulcus (CS) and also having greater activation than the

*Correspondence: j.p.wann@reading.ac.uk

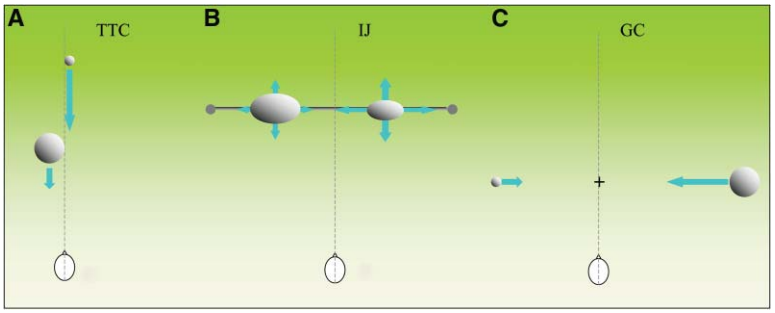

Figure 1. Experimental Stimuli

Aerial view of tasks used, including the position of the observer relative to the virtual objects. Gray dotted lines indicate the midline. The lengths of the blue arrows indicate velocity in (A) and (C) and object expansion rate in (B). (A) Time to collision (TTC). Two balls of randomized size and start distance approached the observer with velocities calculated to produce a 200 ms difference in arrival time. As soon as possible, the observer indicated which ball would arrive first by pressing a button. Judgments were based upon optical size and expansion rate, and it was often the case that the correct response corresponded to the optically smaller object, with the smaller absolute expansion rate but the larger relative expansion rate. (B) Inflation Judgment (IJ). The long gray line with gray circles at each end is the overhead view of an H-shaped frame that supported two oval objects of randomized starting size. The frame remained of a constant size, and the objects did not move during the trial. The blue arrows indicate the absolute rate at which the objects were inflating. The more slowly inflating object expanded at 75% the rate of its faster counterpart. The inflation rate of the more rapidly growing object varied from trial to trial. The observer indicated which object had a faster inflation as quickly as possible. (C) Gap cosure (GC). Two balls of randomized size and distance appeared either side of a central cross and translated toward the center. The speed of translation was calculated to produce a 200 ms difference in arrival time at the center. In judging which ball would arrive first at the center, observers could not base their judgments on distance or speed alone but had to consider both factors jointly. A time limit on responses prevented very late responses from being made on the basis of distance alone.

right hemisphere in the superior precentral sulcus (SpreCS), corresponding to the supplementary motor area (SMA). Bilateral activation in the inferior precentral sulcus (IpreCS) was also observed, and this activation may correspond to the frontal eye fields (FEF). The greater activation in the left hemisphere, compared to baseline, might be attributed to participants using the button box with their right hands for the active-judgment tasks; however, left-hemisphere dominance persists when this is controlled (see below). Motor-cortex activation, compared to baseline, could also be attributed to button pressing, but once again this remains when button pressing is controlled. Activation relative to baseline was also observed in the occipitotemporal ventral stream, located on the lateral and ventral aspects of the occipital lobe. It is in this region that previous studies have identified an area activated by the presentation of objects compared to scrambled-object controls [8, 9], termed the lateral occipital complex (LOC).

The greater part of the activation shown in Figure 2 is not specific to making TTC judgments. Much of it is due to the presence of optical expansion, the appearance and disappearance of objects in the scene, and the need to make decisions and to use a response box. The IJ task was designed to share all these features, including an image-expansion profile that would be similar in terms of its effect on low-level mechanisms. The activation remaining when IJ was subtracted from TTC is shown in Figure 3. To clarify the presentation, we only included voxels that were significantly activated at $p < 0.05$ in the TTC $-$ baseline activation map in the TTC $-$ IJ analysis. This baseline masking technique highlights

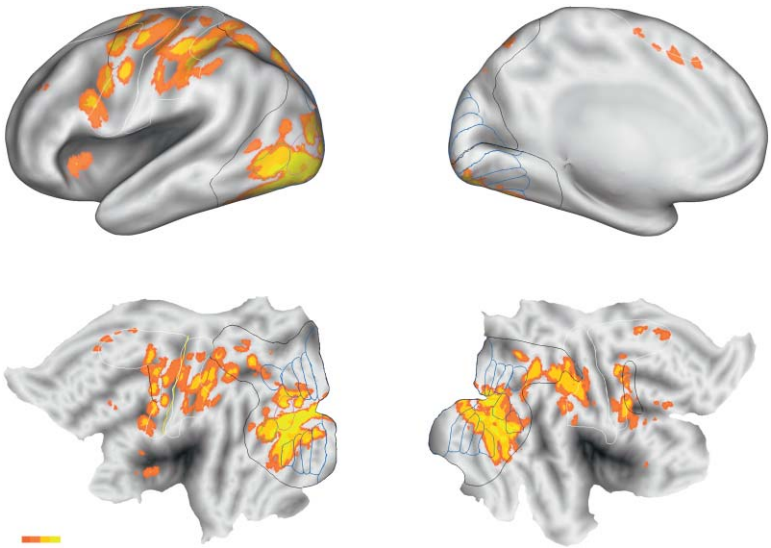

Figure 2. Activation for TTC Minus Resting Baseline Is Shown on Inflated Cortical Surfaces and Flattened Cortical Surfaces

The top left of the figure shows the lateral surface of the left hemisphere; the top right shows the medial surface of the left hemisphere. Flattened cortical surfaces for both hemispheres are shown in the bottom half of the figure. The left hemisphere is shown on the left, and the right hemisphere is shown on the right. On the flattened surfaces, dorsal is up and ventral is down. For both inflated and flattened views, the yellow line shows the position of the central sulcus (CS), and the brown line shows the position of the postcentral sulcus (postCS). The black line indicates the boundary of the visual cortex; the isolated black anterior area corresponds to the frontal eye fields (FEF). The more anterior area bounded in white shows the estimated boundary of motor cortex, whereas the more posterior white area indicates the boundary of the somatosensory cortex. Blue lines indicate the boundaries of retinotopic visual areas. Area LOC is highlighted in pink, and the position of MT+ is highlighted in green. Boundaries were taken from Van Essen et al. [19].

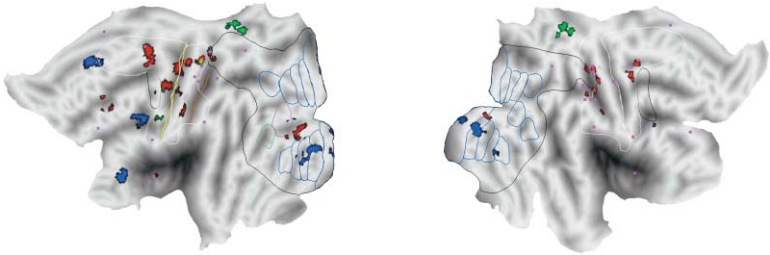

Figure 3. Cross-Condition Contrasts Shown on Flattened Cortical Surfaces

Activation for TTC − IJ is shown in red, GC − IJ in green, and IJ − TTC in blue. Colored borders are as described in the caption for Figure 2. The yellowish activation on the left cortical surface indicates areas shared by the two subtractions. Pink squares show left hemisphere positions of reaching- and grasping-related activation foci from Simon et al. [10]. The foci were taken from Simon et al.'s left-hemisphere activations and warped into the right-hemisphere space because their participants grasped with the right hand only. See text for details.

areas of activation, relative to baseline, in the TTC task and avoids spurious highlighting of areas that were deactivated, relative to baseline, in the IJ condition. The resulting map presents areas specific to the TTC task, when we control for simple image expansion and response requirements. Talairach coordinates and anatomical landmarks for these areas are available in Table S2.

There was only a small amount of TTC-specific activation in the occipital lobe; in the left hemisphere, this activation occurred in the lateral occipital sulcus (LOS) in a non-retinotopic area. In the right hemisphere, a small area of activation remained in the striate cortex. Previous findings indicate that MT+ responds to retinal-image expansion [6], but no TTC-specific activation was found in MT+ when the image-expansion component of the TTC task was subtracted in the IJ control condition. Furthermore, the ventral-stream activation, relative to baseline, that was observed in TTC dropped out when IJ was subtracted from TTC. This activity was most likely driven by the appearance and disappearance, relative to the baseline, of objects in all the tasks used; given the anatomical location, the activity probably corresponds to the LOC.

TTC-specific dorsal-stream activation was strongest in the left hemisphere, where it straddled the sensorimotor areas of parietal and frontal cortex. Bilateral activation was observed at the dorsal end of the postCS, on the border of the visual and somatosensory association cortex. Both hemispheres revealed a number of sites of activation in the somatosensory association cortex. Only the left hemisphere revealed activation in primary somatosensory and motor areas. The location of primary-motor-cortex activity in our group analysis corresponded approximately to the hand and thumb areas of the standard motor homunculus. This result in the group analysis is suggestive, but because individuals show variation in the size and anatomical location of functional areas, it cannot be taken to be true of each individual at this stage. Left-hemisphere activation in the primary somatosensory cortex was positioned on the posterior wall of the CS opposite the motor-cortex activation on the anterior wall of the CS. Because the IJ control task was matched so that it required an identical motor response, these primary sensorimotor activations cannot be attributed to button pressing. It is likely that they were driven by the bilateral TTC-specific activation in the SMA, which projects onto the primary motor cortex. The SMA activity we observed was greater in extent in the left hemisphere. Because SMA projects bilaterally, it may be that the right-hemisphere SMA activity may contribute to the left-hemisphere primary sensorimotor activations. A cluster of three activations of the superior frontal sulcus (SFS) occurred in the left hemisphere only, indicating a specific cognitive component to the TTC task. Finally, a small activation occurred in an area of the left-hemisphere lateral sulcus (LS) normally associated with olfactory and gustatory function. This peculiar result mirrors that of Simon et al. [10], who found activation in the same area for a reaching and grasping task. In fact, six of Simon et al.'s left-hemisphere reaching and grasping activation sites correspond closely to sites that we find to be involved in TTC, as illustrated in Figure 3. Simon et al. acquired their grasping data from pantomimed right-handed grasps, and so these data produced a left-hemisphere-dominant pattern of activation. If an equivalent pattern occurred in the right hemisphere for left-handed grasping, we would once again have notable overlap with the areas activated by our TTC contrast (see Figure 3 for a comparison). Cortical sites found to be involved in intentional reaching and grasping by three further neuroimaging studies also overlap our TTC activations [11–13]. All three studies find activation, similar to our TTC-specific activation, in SMA and primary motor cortex, as well as primary somatosensory and somatosensory association areas. It has also been demonstrated in a study requiring the naming of objects that recalling the names of tools produced dorsal-stream premotor-cortex activity [14]. However, activation of the sensorimotor cortex by simply judging imminent arrival has not been previously demonstrated.

The GC task involved making a TTC judgement for objects that were not moving toward the point of observation. Using an equivalent baseline mask, we subtracted the IJ-task activation from the GC task to see if similar cortical areas were involved in GC and TTC. Results indicated that there was some overlap between task-specific activations in the left hemisphere. However, the majority of active voxels in the GC − IJ contrast lay in a part of the parietal lobe not associated with processing in the TTC task (Figure 3; also Table S3). The overlap areas in the left hemisphere comprised the area on the border of visual and somatosensory association cortex on the posterior side of the postCS, a second overlap in the somatosensory association cortex, and an overlap in the premotor cortex. Additionally, GC pro-

duced a unique premotor cortex activation toward the ventral end of the CS. None of the overlap areas between TTC and GC included the SMA/primary sensorimotor circuit identified as specifically involved in TTC processing in the TTC − IJ contrast. The main activation unique to GC occurred bilaterally in the superior parietal sulcus (SPS) and the marginal ramus of the cingulate sulcus (CiSmr). These are not normally considered to be visual areas but have been associated with cognitive functions.

Activation specific to making judgments about rate of inflation (IJ) revealed by the IJ – TTC contrast was not found in the sensorimotor areas that were specifically activated by the TTC task (Figure 3 and Table S4). Some activation specific to IJ was found in retinotopic areas of the visual cortex. Other activations occurred mainly in the left hemisphere, including an area in orbitofrontal cortex. Primate studies indicate that orbitofrontal cortex receives an input from the temporal-lobe ventral stream visual areas [15], suggesting that performing the IJ task lead to a greater engagement of the ventral visual system than the TTC task. Other areas specifically involved in the IJ task included cognitive and language areas.

Discussion

All three of our motion tasks produced activation, relative to baseline, in the motion-sensitive area MT+. The most likely role of MT+ in a TTC task is to generate a signal related to the rate of optical expansion ($d\theta/dt$), which is present in both the TTC and IJ tasks. In principle, a TTC judgment requires an estimate of the relative rate of expansion ($\theta/[d\theta/dt]$). A subset of neurons that perform this type of processing could be sited within, or bordering, MT+, but at present the spatial limitation of fMRI as a technique prevents precise localization of this function.

The two-stream theory of vision [16] proposes that the ventral visual processing stream is specialized for perception and that the dorsal stream is specialized for action. Of the three tasks our participants performed, only the TTC task contained optical information that could directly specify an action. The action might be an interception (catch) or a defensive response (block), but in either case the balls looming toward the face specified how rapid that response should be. This finding is in tune with the broad concept of affordances [17], whereby particular visual stimuli can map directly to specific actions. In contrast, the IJ and GC tasks contained optical information specifying events in the world that did not afford obvious actions. Only the TTC task produced specific activity in sensorimotor areas that are the target of the dorsal visual system. These activations correspond closely to networks previously identified for reaching and grasping. In the case of reaching and grasping studies, these activations arise from actual movements [10–13]. In our study, the activation cannot be attributed to actual movement or the intention to act. We have reported the results of a group study, and given that functional areas vary in size and location between individuals, only general conclusions can be drawn. In future studies, it will be interesting to functionally localize specific parts of sensorimotor cortex (e.g., the hand region of primary motor cortex) in individuals and then directly measure TTC-related activity in these regions.

Our data contain a number of observations consistent with the two-stream distinction. First, the TTC – baseline contrast shows both dorsal-stream and ventral-stream (LOC) activity, but none of the ventral-stream activity was shown to be specific to TTC processing in the TTC – IJ contrast. Second, the activity specific to IJ revealed by the inverse IJ – TTC subtraction was not located in dorsal-stream sensorimotor areas. Instead, it was found in the orbitofrontal cortex, which has inputs from the ventral visual stream, and in cortex areas associated with language and cognition. Finally, compared to the TTC task, the GC task, which required a judgment of time to arrival in a fronto-parallel plane, produced a much-reduced pattern of activation in sensorimotor areas, as well as its own unique activations.

We conclude that looming patterns that are interpreted as motion in depth toward the observer, and which specify an imminent collision, activate the dorsal-stream systems necessary to prepare an action response. It remains to be established whether this is a response that is automatically activated by any approaching object or whether the engagement of attention to the TTC task is required. Establishing the conditions under which an action response is triggered, or fails to be activated at a neural level, will have major downstream impact for safety systems.

Experimental Procedures

Participants

Participants were six male and six female right-handed volunteers, aged between 20 and 40 years. Participants practiced the three experimental tasks for 5 min per task outside the scanner before being scanned. Each participant undertook a total of four scanning sessions. The first session involved a high-resolution anatomical scan lasting 5 min. Each of the next three sessions presented 175 trials, 3 s in duration, of one of the experimental tasks. These were presented in seven blocks of 25, with a rest period between blocks. The order in which the experimental tasks were performed varied between participants.

Imaging Parameters

Functional MR images were acquired on a Siemens Trio 3T whole-body scanner, with an 8-channel head array coil. EPI parameters were echo time (TE) = 30 ms, repeat time (TR) = 2500 ms, flip angle = 90°, slice thickness = 3 mm, interslice gap = 0, image matrix = 64 × 64, field of view (FoV) = 192 × 192 mm, and functional voxel size 3 × 3 × 3 mm. Forty-six axial slices were acquired in an interleaved sequence covering the whole brain. Prospective motion correction (PACE) was used for tracking any small head movements made by participants, allowing slices to be automatically repositioned between each TR so that they remained in the same position with respect to the participant's head throughout each scanning session.

Each scanning session consisted of 282 TR, lasting 11 min 45 s, plus 12 s of time at the start to allow the signal to stabilize. Each scanning session consisted of seven 75 s blocks of the task, and blocks were separated by 30 s periods of rest. Prior to the first functional MR session, high-resolution anatomical images were acquired in 4 min 32 s (TE = 30 ms, TR = 1960 ms, flip angle = 11°, slice thickness = 3 mm, interslice gap = 0, image matrix = 256 × 256, FOV = 256 × 256 mm, voxel size 1 × 1 × 1 mm, and 176 sagittal slices).

Statistical Analysis

The data from each participant were processed with Statistical Parametric Mapping software (SPM2). The SPM2 motion-correction algorithm was applied to identify any scans in which inter-scan motion had not been negated by PACE prospective-motion correction. No such scans were identified, but one participant's head had moved within a single TR to the extent that the image was distorted. So that the effect of this single scan on the model fit would be minimized, an extra regressor was included in the model for the participant concerned; this regressor had a value of 1 for the volume conserved and 0 for all other volumes in the time series. Volumes from each scanning session were all coregistered to the first volume of the first scan session so that any differences in head position or orientation between sessions would be removed. Normalization to the Montreal Neurological Institute (MNI) template was performed, and spatial smoothing (9 mm) followed. The time series was high-pass filtered with a 210 s cut off, calculated so as not too remove any variance associated with the block design. The activation for each participant was modeled with a linear combination of eight functions obtained by convolving the known temporal profile of the three experimental conditions and the rest blocks with the standard hemodynamic function of SPM, plus its time derivative. Because the TR was relatively short, temporal autocorrelation between volumes was a potential problem, and so the SPM2 correction for serial correlations was applied. Each participant's data were analyzed with t contrasts between each of the conditions and the resting baseline. Contrast maps between the conditions were also created to carry forward to group analysis.

Group analyses were performed with random-effects analyses. The second-level model was a one-way ANOVA design, with nonsphericity correction and adjustment for correlated repeated measures. Results were inspected with t contrasts, with a height threshold corresponding to $p < .0001$ and an extent threshold of 10 voxels. For contrasts between experimental conditions, an inclusive mask was used, such that voxels had to be significantly associated with task $-$ baseline at $p < .05$ before being considered in the contrast. The reasons for this are elaborated in the Results section. Flattened cortical representations of group data were generated with the Computerised Anatomical Reconstruction and Editing Toolkit (CARET v5.1) and the Human Colin Atlas [18, 19].

Visual Stimuli

Stimuli were back projected onto a screen at the back of the bore of the magnet via a Sanyo PLC-XP40L projector operated outside the scanner room and a waveguide. The refresh rate was 75 Hz, and the resolution was 1024 $\times$ 768 pixels. Participants viewed the projection screen via a mirror attached to the head coil. The distance from the projection screen to the mirror was 716 mm, and the distance from the center of the mirror to the participant's eyes was 150 mm. DirectX 8.1 graphics libraries were used to render perspectively correct 2D projections of 3D gray objects against a black background via a simulated light source behind and above the point of observation.

So that final optical size would not be a confound, observers were required to respond as soon as they felt confident in their judgment. On each TTC trial, the simulated diameter of each of the two approaching spherical objects was randomly varied between 48 and 96 cm. Each object had a randomly assigned velocity between 7 and 14 m/s. These randomizations ensured that judgments were based upon processing of the relationship between optical size and expansion rate, rather than confounding variables such as starting optical size or expansion rate alone. Once these parameters were determined, the starting distance of each object was computed so that the TTC with the point of observation for one object would be 1900 ms for one object and 2100 ms for the other. The object height in the scene was set so that the center of the sphere approached the eye directly. The image of an object was occluded once its optical size exceeded 16°. If this occurred, responses were no longer accepted and the trial was considered an incorrect response. Participants were aware of this, and it only occurred on three occasions across all scanning sessions. This rule prevented the final optical size of the objects from being informative about which object would arrive first. Both objects were occluded when the participant responded.

In IJ trials two spherical objects appeared at a simulated distance of 12 m. They appeared suspended on an H-shaped frame, one either side of the participant's midline. The horizontal separation between the centers of the objects was 3.7 m. Their initial diameters varied between 16 and 96 cm. Both objects inflated in the horizontal and vertical dimensions, but the inflation in the horizontal direction was double that in the vertical direction, causing the objects to become increasingly elliptical in shape. The expansion rate in the horizontal dimension of each side of the more rapidly inflating target object was assigned a random value between 0.192 and 0.76 m/s. The expansion rate of the other object was calculated to be 25% slower. The display was erased when a response was made, or after 2 s if no response was made. The participant's task was to indicate which object had the faster expansion rate. On some trials this corresponded to the smaller object because of the difference in initial size. In the IJ task the optical expansion rate of the opposite edges was constant, whereas in the TTC task the optical expansion rate increased as the objects came closer and their optical size increased.

In the GC task objects were created under the same parameters as for the TTC task, except that the initial distances to the left and right of the participant's midline were used in place of the distance from the point of observation. Both objects had a simulated depth of 70 m and translated toward the center of the display with velocities determined as in the TTC condition, producing an arrival-time difference of 200 ms. The center of the display was marked by a fixation cross, and participants indicated which object would reach the cross first. The time at which an object was erased from the display was determined from the optical size of the objects for an imaginary observer at the target position. In initial piloting, the objects were erased when their optical size for the imaginary observer would be 16°, analogous to the TTC task. However, this criterion permitted late judgments to be made on the basis of distance from the center only on trials in which the objects were small. Therefore, we doubled this distance, which ensured that participants used velocity and distance information.

Responses were made by pressing a button with the right hand as soon as the observer was confident of the judgment. The button response immediately caused the screen to be erased. Feedback was provided after each trial by the use of a white square to indicate a correct response and a gray square to indicate an incorrect response. The observers took slightly longer to make their judgments in the TTC task than in the IJ or GC tasks (TTC 1328 ms, IJ 1162 ms, GC 1164 ms; $F_{(2,22)} = 4.01$, $p = 0.03$).

Supplemental Data

Supplemental Data are available at http://www.current-biology.com/cgi/content/full/15/5/453/DC1/.

Received: December 3, 2004
Revised: December 22, 2004
Accepted: December 22, 2004
Published: March 8, 2005

References

1. Lee, D.N. (1976). A theory of visual control of braking based on information about time-to-collision. Perception *5*, 437–459.
2. Wang, Y., and Frost, B.J. (1992). Time to collision is signalled by neurons in the nucleus rotundus of pigeons. Nature *356*, 236–238.
3. Wagner, H. (1982). Flow-field variables trigger landing in flies. Nature *297*, 147–148.
4. Tresilian, J.R. (1999). Visually timed action: Time-out for 'tau'? Trends Cogn. Sci. *3*, 301–310.
5. Rushton, S.K., and Wann, J.P. (1999). Weighted combination of size and disparity: A computational model for timing a ball catch. Nat. Neurosci. *2*, 186–190.
6. Morrone, M.C., Tosetti, M., Montanaro, D., Fiorentini, A., Cioni, G., and Burr, D.C. (2000). A cortical area that responds specifically to optic flow, revealed by fMRI. Nat. Neurosci. *3*, 1322–1328.

7. Todd, J.T. (1981). Visual information about moving objects. J. Exp. Psychol. Hum. Percept. Perform. *7*, 775–810.
8. Malach, R., Reppas, J.B., Benson, R.R., Kwong, K.K., Jiang, H., Kennedy, W.A., Ledden, P.J., Brady, T.J., Rosen, B.R., and Tootell, R.B. (1995). Object-related activity revealed by functional magnetic resonance imaging in human occipital cortex. Proc. Natl. Acad. Sci. USA *92*, 8135–8139.
9. Grill-Spector, K., Kourtzi, Z., and Kanwisher, N. (2001). The lateral occipital complex and its role in object recognition. Vision Res. *41*, 1409–1422.
10. Simon, O., Mangin, J.F., Cohen, L., Le Bihan, D., and Dehaene, S. (2002). Topographical layout of hand, eye, calculation, and language-related areas in the human parietal lobe. Neuron *33*, 475–487.
11. Binkofski, F., Dohle, C., Posse, S., Stephan, K.M., Hefter, H., Seitz, R.J., and Freund, H.J. (1998). Human anterior intraparietal area subserves prehension: a combined lesion and functional MRI activation study. Neurology *50*, 1253–1259.
12. Grafton, S.T., Fagg, A.H., Woods, R.P., and Arbib, M.A. (1996). Functional anatomy of pointing and grasping in humans. Cereb. Cortex *6*, 226–237.
13. Culham, J.C., Danckert, S.L., DeSouza, J.F., Gati, J.S., Menon, R.S., and Goodale, M.A. (2003). Visually guided grasping produces fMRI activation in dorsal but not ventral stream brain areas. Exp. Brain Res. *153*, 180–189.
14. Chao, L.L., and Martin, A. (2000). Representation of manipulable man-made objects in the dorsal stream. Neuroimage *12*, 478–484.
15. Barbas, H. (1993). Organization of cortical afferent input to orbitofrontal areas in the rhesus monkey. Neuroscience *56*, 841–864.
16. Goodale, M.A., and Milner, A.D. (1992). Separate visual pathways for perception and action. Trends Neurosci. *15*, 20–25.
17. Gibson, J.J. 1979. The ecological approach to visual perception. (Boston: Houghton Mifflin).
18. Van Essen, D.C., Drury, H.A., Dickson, J., Harwell, J., Hanlon, D., and Anderson, C.H. (2001). An integrated software suite for surface-based analyses of cerebral cortex. J. Am. Med. Inform. Assoc. *8*, 443–459.
19. Van Essen, D.C. (2004). Organization of visual areas in macaque and human cerebral cortex. In The Visual Neurosciences. L.M. Chalupa and J.S. Werner, Eds. (Cambridge, MA: MIT Press), pp. 507–521.